Materials Science in Semiconductor Processing 97 (2019) 56–61

Contents lists available at ScienceDirect

Materials Science in Semiconductor Processing

journal homepage: www.elsevier.com/locate/mssp

Strain evolution in SiGe-on-insulator fabricated by a modified germanium condensation technique with gradually reduced condensation temperature

Guangyang Lin, Dongxue Liang, Jiaqi Wang, Chunyu Yu, Cheng Li*, Songyan Chen, Wei Huang, Jianyuan Wang, Jianfang Xu

Key Laboratory of Low Dimensional Condensed Matter Physics (Department of Education of Fujian Province), Department of Physics, OSED, Xiamen University, Xiamen, Fujian 361005, PR China

ARTICLE INFO

Keywords:
Ge condensation
SiGe-on-insulator
Condensation temperature
Strain relaxation
Low surface roughness

ABSTRACT

Strain evolution in SiGe-on-insulator fabricated by a modified germanium condensation technique was studied. As enrichment of Ge content, the condensation temperature was proposed to decrease from 1150 to 900 °C through five steps, rather than only two different temperatures (1150 °C and 900 °C) were used as reported previously. Compared to condensation recipe with only two different temperatures, the modified condensation recipe was beneficial to obtain more uniform SiGe layers with lower surface roughness, thus better material quality. As Ge content enriched to 0.54, the strain in SiGe is almost fully relaxed with surface roughness RMS of less than 0.59 nm at condensation temperature of ≥1050 °C. After further condensation at 900 °C, the strain in SiGe accumulated dramatically to −1.23% with a surface roughness RMS of 0.66 nm. At the final stage of Ge condensation process, most of the compressive strain was sustained in Ge-rich SiGe layer. However, when pure GOI was obtained, the compressive strain could be almost fully relaxed by intensive over-oxidation without surface deterioration. The fully relaxed SiGe-on-insulator and germanium-on-insulator with low surface roughness could be a good template for secondary growth of strained Si and Ge, respectively.

Germanium (Ge) is considered as a promising material for silicon-(Si-) based microelectronic and optoelectronic devices for its robust advantage of high carrier mobilities, high absorptance at telecom wavelength (~1550 nm), quasi-direct band structure and compatibility with incumbent Si processing technology. Compared to bulk Ge, Ge-on-insulator (GOI) has greater advantages in both electrical and optical performance. On one hand, the 'on-insulator' structure provides smaller parasitic capacitance and leakage current for electronic devices. On the other hand, the large refractive index difference between Ge and insulator is beneficial to enhance light resonance and confinement in the structure. High-performance MOSFET [1], photodetector [2] and even light emitting devices [3] have been demonstrated based on this platform. Many methods have been proposed to fabricate GOI substrate, such as wafer bonding [4], smart-cut [5], solid-phase crystallization [6,7] and Ge condensation [8]. Among them, Ge condensation method receives abundant researches due to its facility of fabricating ultra thin GOI and SiGe-on-insulator (SGOI) substrates (few to less than 50 nm) [9–12], which is very promising for technology node of 7 nm and beyond. By combination with secondary growth technique [13,14], Ge condensation can be also used to fabricate templates for epitaxy of strained Si [15] and Ge [16] to extend its application fields.

The strain condition in Ge (SiGe) layers can significantly influence the properties of GOI (SGOI) substrates, such as surface roughness [17], bandgap [18] and carrier mobility [19]. For microelectronics devices, it is favorable to sustain large compressive strain in Ge (SiGe) layer to enhance the carrier mobility. While for secondary growth of Si and Ge, it is better to fully relax the strain in Ge (SiGe). To have a better control of the material properties, the strain evolution in SiGe and Ge layers during condensation process should be well understood. The strain condition in SiGe layer is determined by many factors, such as initial strain of SOI [20], Ge content of SiGe [21] before condensation. Previously, we have studied the strain evolution in SiGe layer during the condensation process with two different condensation temperatures (1150 °C for Ge content < 0.40, 900 °C for Ge content > 0.40) [17]. It was suggested that the crystal quality of SiGe layer can be improved through increasing the condensation temperature. Condensation recipe with gradually reduced condensation temperature is preferable. However, few studies were reported for Ge condensation process with gradually reduced temperature [22]. The strain evolution in SiGe layer during Ge condensation with gradually reduced temperature has not

* Corresponding author.
E-mail address: lich@xmu.edu.cn (C. Li).

https://doi.org/10.1016/j.mssp.2019.03.010
Received 3 December 2018; Received in revised form 29 January 2019; Accepted 9 March 2019
Available online 14 March 2019
1369-8001/

been well understood compared to that during Ge condensation with only two different temperatures.

Herein, strain evolution of SiGe-on-insulator fabricated by a modified germanium condensation technique was studied. As Ge content enriched, the condensation temperature was proposed to decrease from 1150 to 900 °C through 5 steps, rather than only two different temperatures (1150 °C and 900 °C) were used as reported previously. The evolutions of strain and surface morphology of SiGe during the modified condensation process were studied by Raman spectroscope and atomic force microscope (AFM), respectively. It is found that the modified condensation recipe is beneficial to improve the material quality. Detailed mechanisms were analyzed and discussed.

The material used for Ge condensation was grown on an 8-inch *p*-type (100) silicon-on-insulator (SOI) wafer with a resistivity of ~10 Ω cm. The SOI wafer was fabricated by separation-by-implanted-oxygen (SIMOX) technology. The thickness of top-Si and buried oxide (BOX) layers is 190 and 120 nm, respectively. The wafer was cleaned by standard Radio Corporation of American (RCA) method and blow-dried with N_2 before loaded into a commercial reduced pressure chemical vapor deposition (RPCVD) chamber. To initiate the growth, the wafer was baked at 1100 °C in H_2 carrier gas to remove the native oxide. Pure silane (SiH_4) and germane (GeH_4) diluted at 10% in H_2 was used as gas source for deposition of Si and Ge atoms, respectively. A silicon buffer layer was firstly grown at 650 °C to obtain a clean epi-ready surface. Next, a uniform $Si_{0.76}Ge_{0.24}$ layer with thickness of 99 nm and a 5-nm Si cap layer were successively grown at 600 °C. The structure diagram of as-grown sample is displayed in Fig. 1(a). Fig. 1(b) shows the X-ray diffraction (XRD) rocking curves of the as-grown sample along (004) and (224) facets, from which a compressive strain of −0.69% ('-' denotes compressive) can be evaluated. Fig. 1(c) exhibits the elemental depth profiles of Ge, Si and O atoms for the as-grown sample taken from Auger energy spectroscope (AES). The uniformity and Ge content of the as-grown structure are validated from the AES data.

The material was cleaved into pieces of 2 × 2 cm^2 before loaded into a 2-inch furnace. Fig. 2 illustrates the detailed modified condensation recipe. The whole condensation process was carried out through seven steps (C0-C6), each of which includes several cycles of 10-mins oxidation and 10-mins annealing. Dry O_2 with purity of 99.5% and N_2 with purity of 99.999% was used as processing gas during oxidation and annealing, respectively. The flow rates were all set as 1.1 L/min. As enrichment of Ge content, the condensation temperature was designed to gradually decrease from 1150 to 900 °C through five steps based on the phase diagram of SiGe alloy [23]. For SiGe with Ge content of < 0.4, 0.4–0.5, 0.5–0.6, 0.6–0.75 and 0.75–1.0, the condensation temperature was initially set as 1150 °C (C0 and C1 steps), 1100 °C (C2 step), 1050 °C (C3 step), 1000 °C (C4 step) and 900 °C (C5 and C6 steps), respectively. During C0 and C1 steps, the samples were pre-oxidized at 900 °C before heated to 1150 °C to prevent Ge loss at high temperature. After C0 step, the surface oxide was removed by buffered oxide etchant (BOE) to prevent self-limiting oxidation effect [24]. The C6 steps were carried out through 6 substeps (C6j, 'j' donates 1–6) to investigate sample evolution at the final stage of Ge condensation process. For comparison, Ge condensation with only two different temperatures (named as "two-step" condensation recipe) was also carried out. For the "two-step" condensation recipe, after C1 step, the condensation temperature of the rest condensation process was directly decreased to 900 °C as reported previously [17]. Raman spectroscope, AFM, and AES were employed to characterize the samples.

Fig. 3(a) shows the Raman spectra of as-grown sample and samples after condensation steps of C0-C5. The signal was excited by a 532-nm laser with a spot size of 4 μm and a power of 28 mW. The following signals were detected for analysis: Si-Si peak (~520 cm^{-1}) from Si, Si-Si (480–510 cm^{-1}), Si-Ge (~400 cm^{-1}) and Ge-Ge peaks (270–300 cm^{-1}) from SiGe. For as-grown sample, Si-Si peak from SiGe is incorporated into that from Si, Ge-Ge and Si-Ge peaks from SiGe are barely observed due to low Ge content. After C0 condensation step, although the intensity of Si-Ge and Si-Si peaks from SiGe increases slightly, Ge-Ge peak is still absent. The result implies that the inter-diffusion effect of Si and Ge atoms overwhelms the Ge condensation effect during C0 step [25]. After C1 condensation step, Ge-Ge mode emerges indicating that condensation effect is dominant during this step due to reduction of SiGe thickness. After C2-C5 condensation steps, Ge-Ge peak intensifies continuously, while Si-Si peaks from SiGe and Si both weaken relatively suggesting continuous enrichment of Ge content in SiGe.

The Ge content (x) and strain ($\varepsilon_{//}$) in SiGe can be quantitatively evaluated from Raman spectra. For SiGe with Ge content of < 0.5, x and $\varepsilon_{//}$ can be calculated from the peak positions of Si-Si (ω_{Si-Si}) and Si-Ge modes (ω_{Si-Ge}) by the equation [26]:

$$\omega_{Si-Si}(cm^{-1}) = 520.6 - 62x - 815\varepsilon_{//}$$
$$\omega_{Si-Ge}(cm^{-1}) = 400.5 + 14.2x - 575\varepsilon_{//}; \quad (1)$$

For SiGe with Ge content of > 0.5, x can be deduced by the equation [27,28]:

$$\frac{I_{Ge-Ge}}{I_{Si-Ge}} = \frac{Bx}{2(1-x)}, \quad (2)$$

where I_{Ge-Ge} and I_{Si-Ge} is the integral intensity of Ge-Ge and Si-Ge peaks, respectively. The coefficient B is determined to be about 1 for our Raman system according to our previous studies [29]. Based on equations (1) and (2), the Ge content of SiGe after C0, C1, C2, C3, C4 and C5 steps was evaluated to be 0.13, 0.35, 0.46, 0.54, 0.59 and 0.78, respectively. Since the total amount of Ge atoms is conserved [30], the thickness of SiGe after C0, C1, C2, C3, C4 and C5 steps was evaluated [31] to be 178, 66, 50, 43, 39 and 30 nm, respectively. The lower Ge content of SiGe after C0 step than that of as-grown sample corroborated that the inter-diffusion effect of Si and Ge atoms overwhelmed the Ge condensation effect during C0 step. Due to conservative oxidation of SiGe, the Ge content of SiGe after each condensation step was lower than the upper limitation of the designed value.

Fig. 3(b) summarizes the evolution of strain in SiGe layer versus Ge

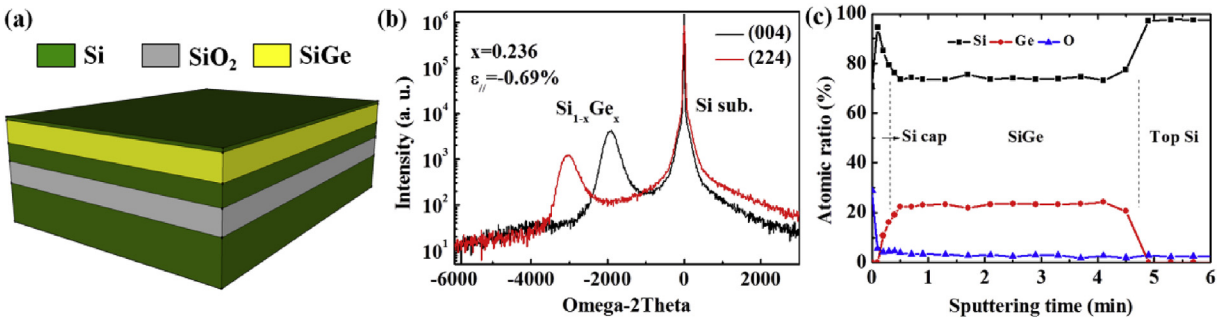

Fig. 1. (a) Structure diagram of the as-grown sample deposited by RPCVD for Ge condensation; (b) (004) and (224) XRD rocking curves and (c) Auger depth profiles of Si, Ge and O atoms for the as-grown sample.

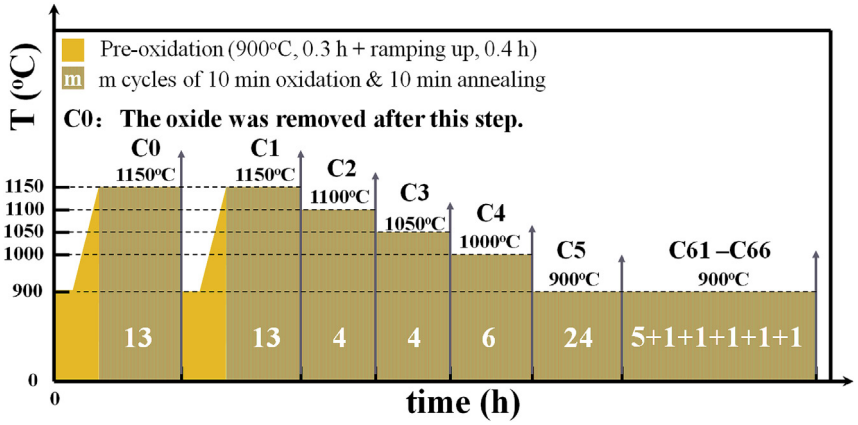

Fig. 2. Modified Ge condensation recipe. As enrichment of Ge content, the condensation temperature was gradually decreased from 1150 to 900 °C through five steps.

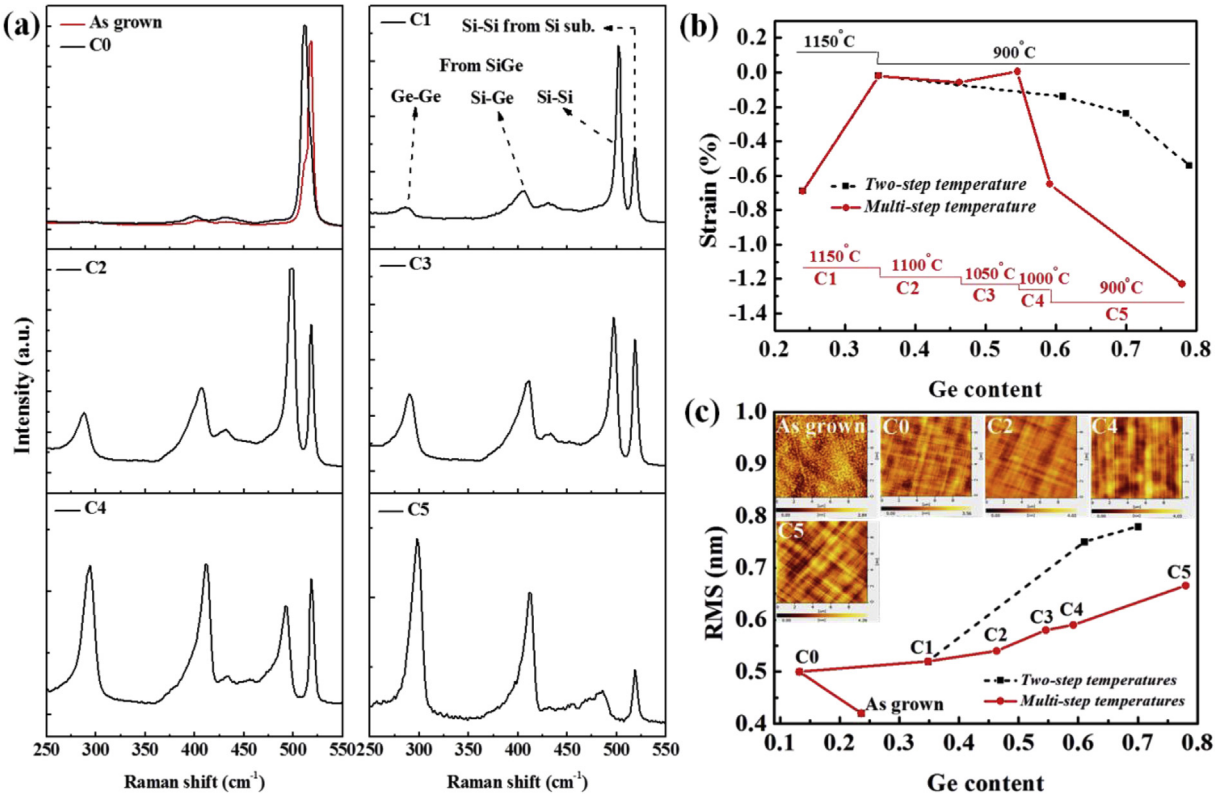

Fig. 3. (a) Evolution of Raman spectra for samples after condensation steps of C0-C5, from which Ge content and strain in SiGe layer can be evaluated; (b) strain variation in SiGe layer versus Ge content after condensation steps of C0-C5 calculated from Raman spectra. The data from "two-step" condensation recipe was also summarized for comparison; (c) dependence of surface roughness RMS of SiGe on Ge content after condensation steps of C0-C5. The result from "two-step" condensation recipe was also included.

content after condensation steps of C0-C5. The strain in SiGe with Ge contents of 0.61, 0.70 and 0.79 fabricated by "two-step" condensation recipe is also presented for comparison. After condensation steps of C0 and C1 at 1150 °C, the compressive strain in SiGe due to lattice mismatch between SiGe and Si is almost fully relaxed through plastic deformation of BOX layer and gliding dislocations along the {111} plane [32]. For SiGe obtained from modified condensation recipe, the strain remains almost fully relaxed after C3 condensation step (Ge content of 0.54, @1050 °C), then dramatically increases to −0.65% after C4 step (Ge content of 0.59, @1000 °C) and −1.23% after C5 step (Ge content of 0.78, @900 °C), respectively. For SiGe obtained by "two-step" condensation recipe, the compressive strain in SiGe increases continuously during the whole investigated condensation process at 900 °C. However, the compressive strain in these SiGe layers is much smaller than that from modified condensation recipe. Even with a Ge content of 0.79, the strain in SiGe obtained by "two-step" condensation recipe is only −0.54%.

To analyze the effect of strain evolution in SiGe layers on the surface morphology of SiGe, AFM images were taken from samples after each condensation step. After removing the surface oxide, areas of $10 \times 10\ \mu m^2$ were randomly selected for scanning. The dependence of surface roughness root mean square (RMS) on Ge content is displayed in Fig. 3(c). For comparison, the result from "two-step" condensation recipe is also exhibited in Fig. 3(c). The surface of initial sample is rather flat with a surface roughness RMS of 0.42 nm. After C0 step, the surface roughness RMS increases to 0.50 nm due to relaxation of lattice

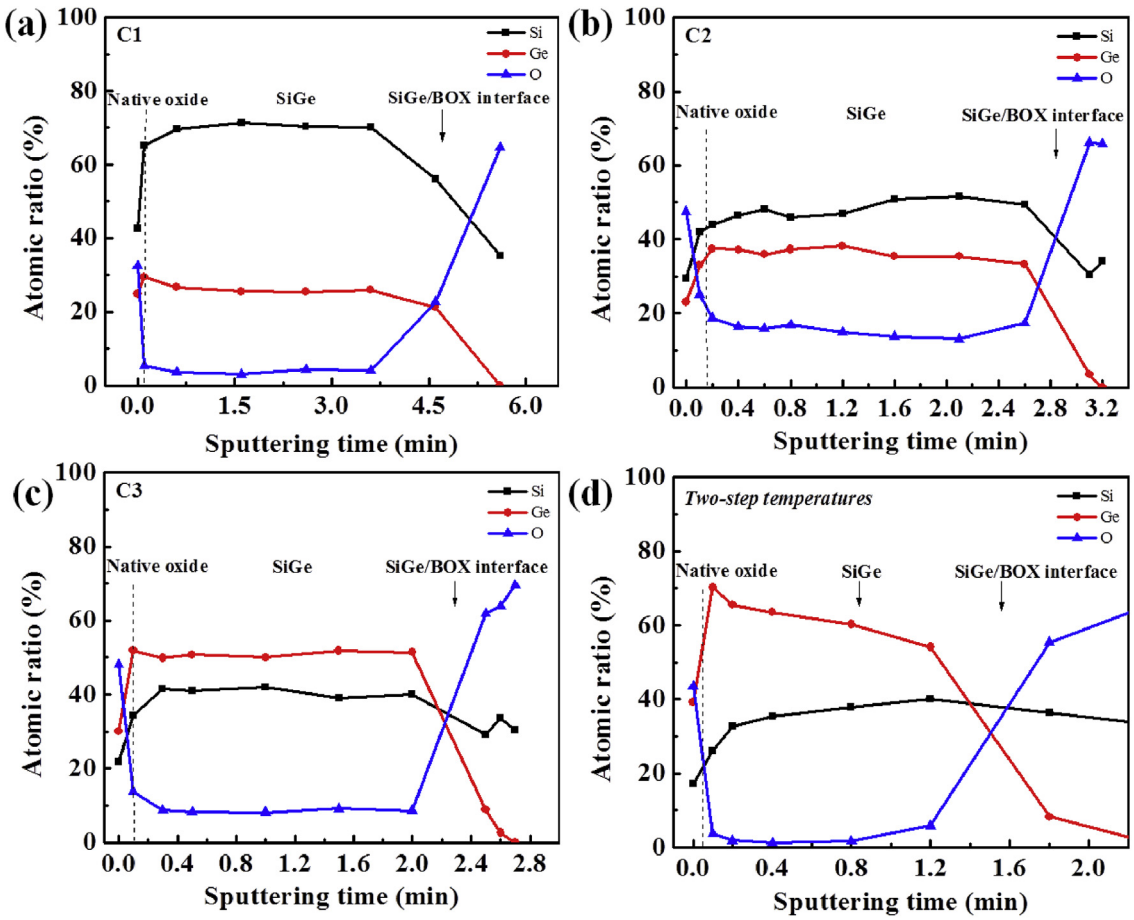

Fig. 4. Si, Ge and O depth profiles of samples obtained by modified condensation recipe after (a) C1, (b) C2, (c) C3 steps and (d) sample obtained by "two-step" condensation recipe taken from Auger electron spectroscopy.

mismatch at 1150 °C. Cross-hatch patterns are observed on sample surface as a result of strain relaxation through gliding dislocations along the {111} planes [32]. After C1 step, the surface roughness RMS increases slightly to 0.52 nm. The evolution of surface morphology for samples obtained by different condensation recipes differs evidently for the rest steps. For samples obtained by "two-step" condensation recipe, the surface roughness RMS dramatically elevates to 0.78 nm after Ge content enriches to 0.70. For SiGe obtained by modified condensation recipe, the surface roughness RMS is much lower. After C2, C3 and C4 steps, the surface roughness RMS is only 0.54, 0.58, and 0.59 nm, respectively. Even after Ge content enriches to 0.78, the surface roughness is less than 0.67 nm. The result suggests that the modified condensation recipe can effectively reduce the surface roughness.

The elemental depth profiles of Si, Ge and O atoms for aforementioned samples were taken by Auger spectroscopy after removal of surface SiO_2. To increase the conductivity of sample surface, samples were fixed on sample stage through covering a carbon conductive tape on sample surface and the stage. Fig. 4(a) and (b) and (c) shows the results of sample after C1, C2 and C3 condensation steps, respectively. For comparison, the result from samples with Ge content of 0.61 obtained by "two-step" condensation recipe is presented in Fig. 4(d). The distribution of Si and Ge atoms in SiGe layers is determined by the competitive effect of Ge condensation and inter-diffusion of Si and Ge atoms. The uniform SiGe layer obtained after C1 step (Fig. 4(a)) is resulted from the fact that the inter-diffusion of Si and Ge atoms overwhelms the Ge condensation effect at 1150 °C. According to previous report, the activation energy of Ge diffusion in Si is 5.8 eV [33], while the activation energy of O_2 diffusion in SiO_2 is 1.17 eV [34]. This means that the inter-diffusion of Ge and Si atoms is more sensitive to condensation temperature. For the "two-step" condensation recipe, the condensation temperature is directly lowered to 900 °C after C1 step. The condensation effect would preponderate the inter-diffusion of Ge and Si atoms consequently. Even with an interval of 10-mins' annealing between oxidation process, large concentration gradient is observed in Ge depth profile, as shown in Fig. 4(d). According to previous study, the large gradient of Ge profile in SiGe layer would lead to generation of dislocations along with strain relaxation [25]. Thus, the large gradient of Ge profile in SiGe layer is undesired. For samples with modified condensation recipe, the condensation temperature reduces gradually from 1150 to 900 °C through five steps. Due to continuous reduction of SiGe thickness and insertion of annealing process during the condensation process, the inter-diffusion of Si and Ge is not affected significantly. Consequently, uniform SiGe layers are obtained after C2 (Fig. 4(b)) and C3 (Fig. 4(c)) steps, which is beneficial to improve the material quality. The O concentrations in samples after C2 and C3 steps are abnormal high due to organic contamination from the carbon conductive tape. For the rest condensation steps, uniform SiGe layers can be sustained due to reduction of SiGe thickness and oxidation speed of SiGe layers [17].

Germanium condensation steps of C61-C66 were designed to investigate sample evolutions at the final stage of Ge condensation process. Fig. 5(a) displays the evolution of Raman spectra for SiGe layers at the final stage of Ge condensation process. A close-up of Ge-Ge and Si-Ge modes is shown in the insets of Fig. 5(a). As Ge condensation proceeds, the intensity of Si-Ge mode gradually diminishes compared to that of Ge-Ge mode and a gradual red shift of ω_{Si-Ge} is observed. From equation (1), ω_{Si-Ge} is proportional to x, under a constant $\varepsilon_{//}$. The red shift of ω_{Si-Ge} means an increase of $\varepsilon_{//}$. Since SiGe layer sustains

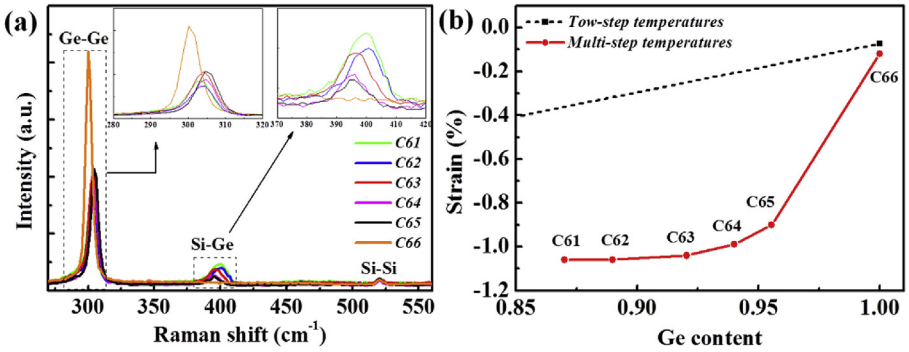

Fig. 5. (a) Raman spectra of samples after condensation steps of C61-C66. A close-up of Ge-Ge and Si-Ge modes is shown in the insets; (b) strain evolution of samples after condensation steps of C61-C66.

compressive strain ($\varepsilon_{//} < 0$), The increase of $\varepsilon_{//}$ indicates a gradual relaxation of compressive strain in SiGe layer. After C66 process, the Si-Ge mode disappears and a pronounced red shift of Ge-Ge mode is observed suggesting formation of pure GOI and a significant strain relaxation process. The thickness of final GOI is evaluated to be 24 nm. Based on equation (2), the Ge content after condensation steps of C61-C66 is evaluated to be 0.87, 0.89, 0.92, 0.94, 0.95 and 1.0, respectively. Detailed strain evolution of these samples is concluded in Fig. 5(b). With a Ge content of 0.87, the −1.23% compressive strain observed in SiGe layer after C5 step is relaxes to −1.06%. After C61 to C65 condensation steps, the compressive strain only gradually reduces from −1.06% to −0.90%. However, upon acquisition of pure GOI substrate after C66 step, the −0.90% compressive strain dramatically relaxes to −0.12%. For GOI substrate obtained by "two-step" condensation recipe, the compressive strain has relaxed to −0.073% due to over oxidation of the GOI substrate.

Fig. 6 shows the variation of surface roughness RMS for samples after C61-C66 steps. Due to strain relaxation, the surface roughness RMS has elevated from 0.66 to 0.87 nm after C61 condensation step. After C62-C65 steps, since the compressive strain does not relax significantly, the surface roughness RMS only increases slightly with a fluctuation between 0.9 and 1.0 nm. After C66 steps, although the compressive strain relaxes dramatically, the surface roughness RMS is still only 0.94 nm. This implies that the mechanism of strain relaxation in the final GOI is different from that in SGOI. From the AFM image of the GOI substrate (inset in Fig. 6), some disordered lines, which are originated from dislocation loops [35], are observed due to over-oxidation of the GOI substrate. According to pervious report, Ge atoms will

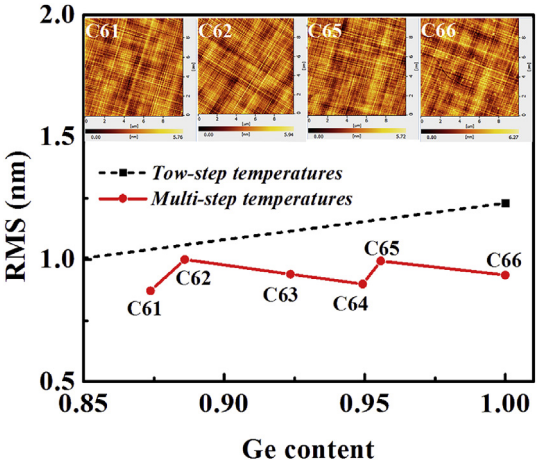

Fig. 6. Dependence of surface roughness RMS of samples after condensation steps from C61 to C66. The data from "two-step" condensation recipe is also presented for comparison.

move out from crystalline position to accommodate the approaching oxygen atoms. The compressive strain in GOI would dramatically relax through over oxidation consequently [36]. While for GOI substrate obtained by Ge "two-step" condensation recipe, the surface roughness RMS has deteriorated to 1.23 nm after over oxidation.

Aforementioned analyses manifest that the proposed modified condensation recipe has more advantages over the "two-step" condensation recipe in improving the material quality of fabricated SGOI and GOI substrates. At 1150 °C, uniform low Ge content $Si_{1-x}Ge_x$ layers ($x < 0.35$) with almost fully relaxed strain can be obtained due to stronger inter-diffusion effect of Si and Ge atoms than Ge condensation effect. For the "two-step" condensation recipe, the condensation temperature is directly decreased from 1150 to 900 °C during the rest condensation process. The condensation effect overwhelms the inter-diffusion effect of Si and Ge atoms leading to gradual formation of nonuniform SiGe layers. Since the plastic deformation of BOX layer can be neglected at 900 °C, which is lower than the viscous flow temperature of SiO_2 (~965 °C) [37], the compressive strain in SiGe layers accumulates gradually. However, the large gradient of Ge profile in SiGe layer would facilitate generation of dislocations [25]. Most of the compressive strain is relaxed through gliding dislocations along {111} planes along with deterioration of surface roughness. The maximum compressive strain that can be sustained in SiGe layers is only −0.54%. Through gradually reducing the condensation temperature from 1150 to 900 °C, sufficient inter-diffusion of Si and Ge is assured during the whole condensation process resulting in formation of uniform SiGe layers. After Ge content enriches to 0.54 at 1050 °C, the strain is still almost fully relaxed. The compressive strain mainly relaxes through deformation of the BOX layer, thus the surface is quiet smooth with a roughness RMS of only 0.58 nm. The high quality relaxed SiGe layers can be used as a template for secondary growth of strained Si. As condensation temperature reduces below 1050 °C, the effect of strain relaxation through deformation of BOX layer becomes weaker and even can be neglected. Additionally, the uniform distribution of Si and Ge atoms alleviates generation of dislocations [25]. Hence, after Ge content enriches from 0.54 (@1050 °C) to 0.78 (@900 °C), the compressive strain dramatically accumulates to −1.23% with a surface roughness of 0.67 nm. At the final stage of Ge condensation process, most of the compressive strain is sustained in SiGe layers, which are supposed to have enhanced carrier mobility. The highly-compressive SiGe with high Ge content is very promising to be used as active channel for MOSFET. After acquisition of pure GOI substrate, the large compressive strain is almost fully relaxed due to additional oxidation of the material. With the modified condensation recipe, the surface roughness RMS of final GOI substrate is reduced by ~0.3 nm (0.94 nm) compared to that from the "two-step" condensation recipe. The relaxed GOI substrate can be a good template for secondary growth of Ge. Overall, the modified condensation recipe is beneficial to obtain more uniform SiGe layers with lower surface roughness, larger maximum compressive strain and less

dislocations, thus better material quality. The modified condensation recipe is preferably employed to fabricate SGOI and GOI substrates.

In summary, we have studied the strain evolution in SiGe-on-insulator fabricated by a modified germanium condensation technique. The condensation temperature was proposed to decrease from 1150 to 900 °C through five steps during the condensation process, rather than only two different temperatures (1150 °C and 900 °C) were used as reported previously. From AES depth profiles, it was found that uniform SiGe layers could be obtained by the modified condensation recipe. As Ge content enriched to 0.54, the strain in SiGe is almost fully relaxed with surface roughness RMS of less than 0.59 nm at condensation temperature of ≥1050 °C. After further condensation at 900 °C, large compressive strain (up to −1.23%) would be sustained in SiGe with Ge content of 0.78 and surface roughness RMS of 0.66 nm. Compared to condensation recipe with only two different temperatures, the modified condensation recipe was beneficial to obtain more uniform SiGe layers with lower surface roughness, larger maximum compressive strain and less dislocations, thus better material quality. At the final stage of Ge condensation process, as further enrichment of Ge content, most of the compressive strain was sustained in the Ge-rich SiGe layers. However, when pure GOI was obtained, the compressive strain could be almost fully relaxed by intensive over-oxidation without surface deterioration. The fully relaxed SiGe-on-insulator and germanium-on-insulator with low surface roughness could be a good template for secondary growth of strained Si and Ge, respectively.

Acknowledgements

This work was supported by the National Natural Science Foundation of China under grant No. 61474094, 61176092, and the National Basic Research Program of China under grant No. 2013CB63210.

References

[1] L. Hutin, C.L. Royer, J. Damlencourt, J. Hartmann, H. Grampeix, V. Mazzocchi, C. Tabone, B. Previtali, A. Pouydebasque, M. Vinet, O. Faynot, GeOI pMOSFETs scaled down to 30-nm gate length with record off-state current, IEEE Electron. Device Lett. 31 (3) (2010) 234–236.
[2] S. Assefa, F. Xia, S.W. Bedell, Y. Zhang, T. Topuria, P.M. Rice, Y.A. Vlasov, CMOS-integrated high-speed MSM germanium waveguide photodetector, Opt. Express 18 (5) (2010) 4986–4999.
[3] J.R. Jain, A. Hryciw, T.M. Baer, D.A.B. Miller, M.L. Brongersma, R.T. Howe, A micromachining-based technology for enhancing germanium light emission via tensile strain, Nat. Photon. 6 (2012) 398.
[4] J.R. Jain, D.-S. Ly-Gagnon, K.C. Balram, J.S. White, M.L. Brongersma, D.A.B. Miller, R.T. Howe, Tensile-strained germanium-on-insulator substrate fabrication for silicon-compatible optoelectronics, Opt. Mater. Express 1 (6) (2011) 1121–1126.
[5] C. Deguet, C. Morales, J. Dechamp, J.M. Hartmann, A.M. Charvet, H. Moriceau, F. Chieux, A. Beaumont, L. Clavelier, V. Loup, N. Kernevez, G. Raskin, C. Richtarch, F. Allibert, F. Letertre, C. Mazure, Germanium-on-insulator (GeOI) structures realized by the Smart Cut/spl trade/technology, 2004 IEEE International SOI Conference, 2004, pp. 96–97 (IEEE Cat. No.04CH37573).
[6] D. Takahara, R. Yoshimine, T. Suemasu, K. Toko, High-hole mobility Si1-xGex (0.1 ≤ x ≤ 1) on an insulator formed by advanced solid-phase crystallization, J. Alloy. Comp. 766 (2018) 417–420.
[7] Y. Ryota, M. Kenta, S. Takashi, T. Kaoru, Advanced solid-phase crystallization for high-hole mobility (450 cm 2 V −1 s −1) Ge thin film on insulator, APEX 11 (3) (2018) 031302.
[8] S. Nakaharai, T. Tezuka, N. Sugiyama, Y. Moriyama, S.-i. Takagi, Characterization of 7-nm-thick strained Ge-on-insulator layer fabricated by Ge-condensation technique, Appl. Phys. Lett. 83 (17) (2003) 3516–3518.
[9] H. Norio, M. Yoshihiko, Nakaharai Shu, Toshifumi Irisawa, Naoharu Sugiyama, T. Shin-ichi, Deformation induced holes in Ge-rich SiGe-on-Insulator and Ge-on-Insulator substrates fabricated by Ge condensation process, APEX 1 (10) (2008) 101401.
[10] S. Nakaharai, T. Tezuka, N. Hirashita, E. Toyoda, Y. Moriyama, N. Sugiyama, S. Takagi, Formation process of high-purity Ge-on-insulator layers by Ge-condensation technique, J. Appl. Phys. 105 (2) (2009) 024515.
[11] V. Boureau, D. Benoit, B. Warot, M. Hÿtch, A. Claverie, Strain/composition interplay in thin SiGe layers on insulator processed by Ge condensation, Mater. Sci. Semicond. Process. 42 (2016) 251–254.
[12] T. David, J.-N. Aqua, K. Liu, L. Favre, A. Ronda, M. Abbarchi, J.-B. Claude, I. Berbezier, New strategies for producing defect free SiGe strained nanolayers, Sci. Rep. 8 (1) (2018) 2891.
[13] M. Bosi, G. Attolini, M. Calicchio, C. Ferrari, C. Frigeri, E. Gombia, A. Motta, F. Rossi, Homoepitaxial growth of germanium for photovoltaic and thermophotovoltaic applications, J. Cryst. Growth 318 (1) (2011) 341–344.
[14] J. Wang, L. Shen, G. Lin, J. Wang, J. Xu, S. Chen, G. Xiang, C. Li, Homoepitaxy of Ge on ozone-treated Ge (1 0 0) substrate by ultra-high vacuum chemical vapor deposition, J. Cryst. Growth 507 (2019) 113–117.
[15] M.L. Lee, E.A. Fitzgerald, M.T. Bulsara, M.T. Currie, A. Lochtefeld, Strained Si, SiGe, and Ge channels for high-mobility metal-oxide-semiconductor field-effect transistors, J. Appl. Phys. 97 (1) (2004) 011101.
[16] L. Souriau, V. Terzieva, W. Vandervorst, F. Clemente, B. Brijs, A. Moussa, M. Meuris, R. Loo, M. Caymax, High Ge content SGOI substrates obtained by the Ge condensation technique: a template for growth of strained epitaxial Ge, Thin Solid Films 517 (1) (2008) 23–26.
[17] G. Lin, X. Lan, N. Chen, C. Li, D. Huang, S. Chen, W. Huang, J. Xu, H. Lai, Strain evolution of SiGe-on-insulator fabricated by germanium condensation method with over-oxidation, Mater. Sci. Semicond. Process. 56 (2016) 282–286.
[18] X. Sun, J. Liu, L.C. Kimerling, J. Michel, Toward a germanium laser for integrated silicon photonics, IEEE J. Sel. Top. Quantum Electron. 16 (1) (2010) 124–131.
[19] F. Murphy-Armando, S. Fahy, Giant enhancement of n-type carrier mobility in highly strained germanium nanostructures, J. Appl. Phys. 109 (11) (2011) 113703.
[20] T. Tezuka, N. Hirashita, Y. Moriyama, S. Nakaharai, N. Sugiyama, S.-i. Takagi, Strain analysis in ultrathin SiGe-on-insulator layers formed from strained Si-on-insulator substrates by Ge-condensation process, Appl. Phys. Lett. 90 (18) (2007) 181918.
[21] S. Takagi, K. Tomiyama, S. Dissanayake, M. Takenaka, Critical factors for enhancement of compressive strain in SGOI layers fabricated by Ge condensation technique, ECS Trans. 33 (6) (2010) 501–509.
[22] J. Suh, R. Nakane, N. Taoka, M. Takenaka, S. Takagi, Effects of additional oxidation after Ge condensation on electrical properties of germanium-on-insulator p-channel MOSFETs, Solid State Electron. 117 (2016) 77–87.
[23] R.W. Olesinski, G.J. Abbaschian, The Ge-Si (Germanium-Silicon) system, Bull. Alloy Phase Diagr. 5 (2) (1984) 180–183.
[24] Y. Zhang, C. Li, K. Cai, Y. Chen, S. Chen, H. Lai, J. Kang, Experimental evidence of oxidant-diffusion-limited oxidation of SiGe alloys, J. Appl. Phys. 106 (6) (2009) 063508.
[25] N. Sugiyama, T. Tezuka, T. Mizuno, M. Suzuki, Y. Ishikawa, N. Shibata, S. Takagi, Temperature effects on Ge condensation by thermal oxidation of SiGe-on-insulator structures, J. Appl. Phys. 95 (8) (2004) 4007–4011.
[26] J.C. Tsang, P.M. Mooney, F. Dacol, J.O. Chu, Measurements of alloy composition and strain in thin GexSi1 − x layers, J. Appl. Phys. 75 (12) (1994) 8098–8108.
[27] P.M. Mooney, F.H. Dacol, J.C. Tsang, J.O. Chu, Raman scattering analysis of relaxed GexSi1 − x alloy layers, Appl. Phys. Lett. 62 (17) (1993) 2069–2071.
[28] H.K. Shin, D.J. Lockwood, J.M. Baribeau, Strain in coherent-wave SiGe/Si superlattices, Solid State Commun. 114 (10) (2000) 505–510.
[29] C. Yanghua, L. Cheng, L. Hongkai, C. Songyan, Quantum-confined direct band transitions in tensile strained Ge/SiGe quantum wells on silicon substrates, Nanotechnology 21 (11) (2010) 115207.
[30] Q.T. Nguyen, J.F. Damlencourt, B. Vincent, L. Clavelier, Y. Morand, P. Gentil, S. Cristoloveanu, High quality Germanium-On-Insulator wafers with excellent hole mobility, Solid State Electron. 51 (9) (2007) 1172–1179.
[31] S. Huang, W. Lu, C. Li, W. Huang, H. Lai, S. Chen, A CMOS-compatible approach to fabricate an ultra-thin germanium-on-insulator with large tensile strain for Si-based light emission, Opt. Express 21 (1) (2013) 640–646.
[32] M. Tanaka, I. Tsunoda, T. Sadoh, T. Enokida, M. Ninomiya, M. Nakamae, M. Miyao, Thickness-dependent stress-relaxation in thin SGOI structures and its improvement, Thin Solid Films 508 (1) (2006) 247–250.
[33] M. Ogino, Y. Oana, M. Watanabe, The diffusion coefficient of germanium in silicon, Phys. Status Solidi 72 (2) (1982) 535–541.
[34] D.R. Hamann, Diffusion of atomic oxygen in SiO2, Phys. Rev. Lett. 81 (16) (1998) 3447–3450.
[35] H.H. Silvestri, H. Bracht, J.L. Hansen, A.N. Larsen, E.E. Haller, Diffusion of silicon in germanium, AIP Conf. Proc. 772 (1) (2005) 97–98.
[36] C. Mastail, I. Bourennane, A. Estève, G. Landa, M.D. Rouhani, N. Richard, A. Hémeryck, Oxidation of Germanium and Silicon surfaces (100): a comparative study through DFT methodology, IOP Conf. Ser. Mater. Sci. Eng. 41 (1) (2012) 012007.
[37] E.P. EerNisse, Viscous flow of thermal SiO2, Appl. Phys. Lett. 30 (6) (1977) 290–293.